Structural Analysis of Charge Transfer Salts from Synchrotron X-ray and Neutron Powder Diffraction Data

A thesis submitted in partial fulfillment of the requirements for the degree of Bachelor of Science in Physics from the College of William and Mary

by

Sahnun Hassan Mohamud

Advisor: Dr. Silvina Pagola

Senior Research Coordinator: Dr. Gina Hoatson

Date: May 11, 2015

Table of Contents:

Abstract

This research work has been motivated by my interest in the chemical synthesis and study of the solid state properties of new materials. More specifically, two charge transfer salts of the electron donor tetrathiafulvalene (TTF) and chemical derivatives of benzoquinones (electron acceptors), have been studied. The materials were synthesized by mechanochemistry, grinding the powders of the reactants in presence of small quantities of different solvents. This synthesis method leads to different crystal structures (or polymorphs) of the products, which show different physical properties. The charge transfer salts under study were TTF-*o*-CA (*o*-CA is *o*-chloranil) and TTF-2,5-dichloro-*p*-benzoquinone. The refined lattice parameters of the latter compound are a = 6.8418(2) Å, b = 7.21331(17) Å, c = 7.9348(2) Å, α = 93.618(2)˚, β = 97.6267(19)˚ and γ = 106.9407(19)˚. The unit cell volume is 369.147(17) Å^3 and the space group is $P\bar{1}$ (triclinic). TTF-2,5-dichloro-*p*-benzoquinone is made of columnar stacks of alternating TTF and 2,5-dichloro-*p*-benzoquinone molecules running along a direction parallel to the crystallographic b-axis. The combined analysis of the synchrotron X-ray and neutron powder diffraction data of this material resulted in a set of bond distances and bond angles for the TTF molecules, which gave rise to an estimated charge transferred (ρ) between donors and acceptors of ~0.36 e$^-$.

1. Introduction

The Greek philosopher Democritus has been credited as having the earliest recorded speculation of the atom's existence, which he believed to be an indivisible unit and therefore a fundamental basis of all matter in the universe.[1] Democritus did very well for someone who did not have access to modern scientific tools for "seeing" deeply into the nature of matter, and clever scientists after him have worked enormously hard to find ways to probe deeper into the fundamental nature of matter beyond the naked eye, which has a resolution suitable for viewing objects which scatter visible light wavelengths (4000-7000 Å). Atomic radii are in the order of 1 Å (10^{-10} m), thus to be able to similarly "see" atoms, wavelengths much shorter than those of visible light are required. The discovery of the diffraction of X-rays from solids by the German physicist Max Von Laue in 1912 represented an extraordinary step forward in this aim.[2] Laue hypothesized that by passing an X-ray beam through a crystalline solid, the X-rays would interfere and this would result in a diffraction pattern due to the periodic arrangement of atoms within crystalline solids, thereby providing proof of both, the wave nature of X-rays and the spatial arrangement of atoms at regular intervals in crystals.

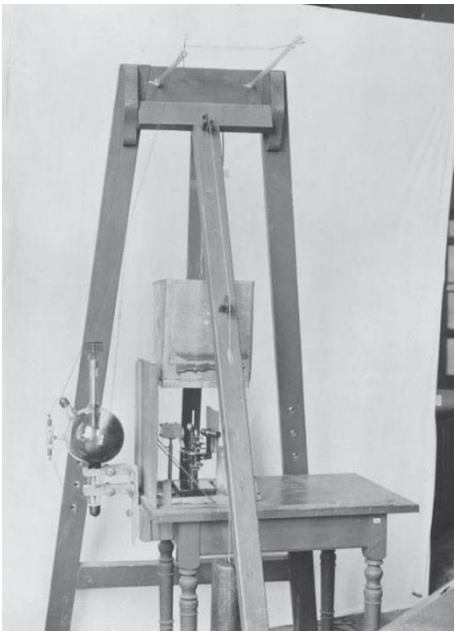

Figure 1: The apparatus used for the discovery of X-ray diffraction in crystals, exhibited at Deutsches Museum in Munich, Germany. Figure reproduced from citation 2.

X-ray diffraction from single crystals has since become a leading method in determining the crystal structures for a vast range of materials. A defined "structure" means different things

to different people, and in crystallography it simply means having knowledge of the atomic arrangement (*e.g.,* relative positions, bond distances, bond angles) in the most basic building block of a crystal (formally known as the unit cell) which can be translated in space to form a complete crystal. Thanks to technological advances over the past two decades, chiefly the widespread availability of computers and open source crystallography software, even for crystal structure determination from powders, [3] structures are typically completed in a matter of hours or days! Moreover, through the use of databases containing powder diffraction patterns and detailed structural information of thousands of organic and inorganic compounds, solid state chemists and physicists are able to rapidly identify crystalline materials by comparing their diffraction patterns to the collection of powder diffraction patterns in the database. Knowledge of the structures of materials is among the primary objectives of chemistry and the material sciences, since it allows the study of the chemical bonding in solids and the formulation of structure-properties relationships. Finally, it is worth noting that crystallography is routinely applied in many vital and economically significant industries today, such as pharmaceuticals, minerals, computers, aeronautical, automobile, agricultural and food industries.

The main objective of this project has been to characterize the crystal structures of two newly synthesized charge transfer salts, TTF-2,5-dichloro-*p*-benzoquinone and TTF-*o*-CA. The structure of TTF-2,5-dichloro-*p*-benzoquinone has been used to calculate the bond lengths in tetrathiafulvalene and infer features of its chemical bonding. The use of empirical formulas afforded the calculation of the charge transferred (ρ) among tetrathiafulvalene and the 2,5-dichloro-*p*-benzoquinone electron acceptor.

The Powder Diffraction Method

The question of how we can ”see” individual atoms and molecules, either directly or indirectly, has been answered by the diffraction methods. As mentioned earlier, the naked human eye which operates by detecting scattered visible light waves is incapable of viewing atoms due to visible light wavelengths are much longer than atomic radii. X-rays are able to diffract from crystals since their wavelengths are on the order of 0.1 Å – 100 Å. Thus, a suitable detector to measure the X-rays scattered from atoms in crystals and a way of interpreting the resultant diffraction pattern, is in principle all one needs to characterize the structure of any crystalline solid.

The fundamental aspects of the powder diffraction method are illustrated in figure 2. Incident radiation on a powder sample results in the formation of cones of diffracted X-rays, schematically represented in figure 2(a). In a powder diffractometer, the X-ray source (or the sample stage) rotates at an angle θ as shown in figure 2(b). The diffracted X-ray intensities are recorded by the detector as a set of peaks of diffracted radiation (X-ray counts) *vs.* 2θ angles (in degrees) as shown in figure 2(c).

The powder diffraction method was independently developed by Debye and Scherrer in Germany in 1916, and in the USA by Hull in 1917.[3] Over the course of the next 50 years, the “traditional” applications, which include crystal phase identification, determination of accurate lattice parameters, and the analysis of structural imperfections, were well established.[3] In 1967 the power of the method was significantly augmented with the introduction by Hugo Rietveld of a method for refining crystal structures from neutron powder diffraction data. Since then, the Rietveld method has been used extensively in deriving structural information from powder data, thus entering the once exclusive domain of single crystal diffraction methods.

Figure from http://chemwiki.ucdavis.edu/Analytical_Chemistry/Instrumental_Analysis/Diffraction/Powder_X-ray_Diffraction

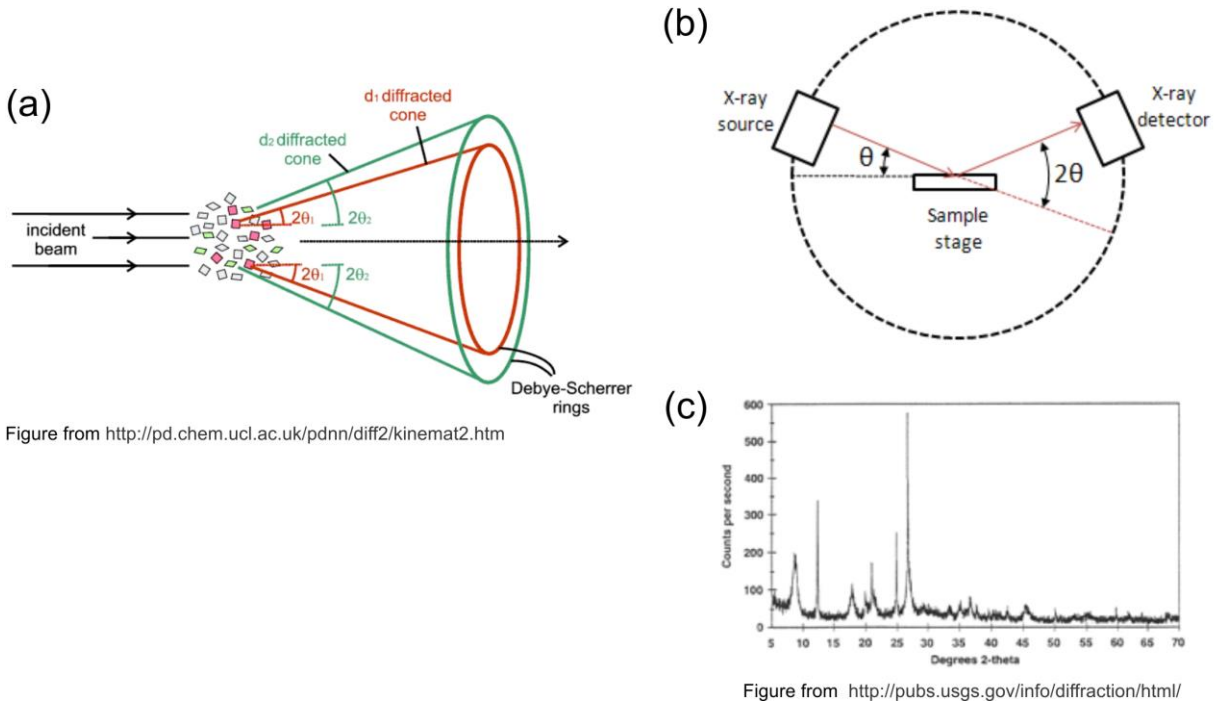

Figure from http://pd.chem.ucl.ac.uk/pdnn/diff2/kinemat2.htm

Figure from http://pubs.usgs.gov/info/diffraction/html/

Figure 2: (a) X-ray radiation incident on a powder produces Debye-Scherrer diffraction cones of diffracted radiation at 2θ angles from the incident beam direction. (b) Schematic arrangement of the X-ray source, the sample holder and the X-ray detector in a powder diffraction experiment. (c) A typical X-ray powder diffraction data showing peaks of diffracted X-ray radiation *vs.* the 2θ angle. The peaks are measured when the detector intercepts the cones.

X-rays and neutrons can both serve as a radiation source for the powder diffraction method. Synchrotron powder diffraction is often referred to as high resolution X-ray powder diffraction due to the smaller instrumental contribution to the peak widths, than that from conventional X-ray diffractometers. The advantages, disadvantages and generation technique for each radiation source are summarized in table 1.

Table 1: Comparison of radiation sources in powder diffraction, their generation technique, strengths and limitations.

Radiation Source	**Strengths**	**Limitations**	**Generation technique**
Neutron	* The location of light atoms in presence of heavier atoms. * Differentiation between adjacent elements in the periodic table. * Determination of the spin arrangements in magnetically ordered materials. * Diffraction data measurable up to relatively large diffraction angles. * In-situ studies varying temperature or pressure are possible.	* Neutron sources are expensive to maintain. * A relatively large amount of sample is required (in the order of 1 gram), which is an obstacle for costly or difficult to obtain specimens.	* Nuclear reactors (most common). * Spallation from metal targets bombarded with high energy (approximately 500 MeV) protons.

Synchrotron	* The instrumental contribution to peak broadening is minimal. * High incident X-ray intensity. * The wavelength is tunable, affording studies close to the X-ray absorption borders, or far from them minimizing X-ray absorption or fluorescence. * In-situ studies varying temperature or pressure and time-dependent studies are possible.	* Poor signal to noise ratio at high diffraction angles due to fall-off of the X-ray atomic scattering factors.	* From electrons travelling at relativistic velocities deflected by magnetic fields in a synchrotron.
Conventional (sealed X-ray tube and rotating anode sources).	* Simple and relatively maintenance free assembly.	* The overall efficiency of the X-ray source is low (approximately 1%).	* X-ray tubes, where electromagnetic radiation is generated from the impact of high energy electrons with a metal target, typically Cu and Mo.

Figure 3 shows the arrangement of the radiation source, the sample and the detector in the instruments used in this study.

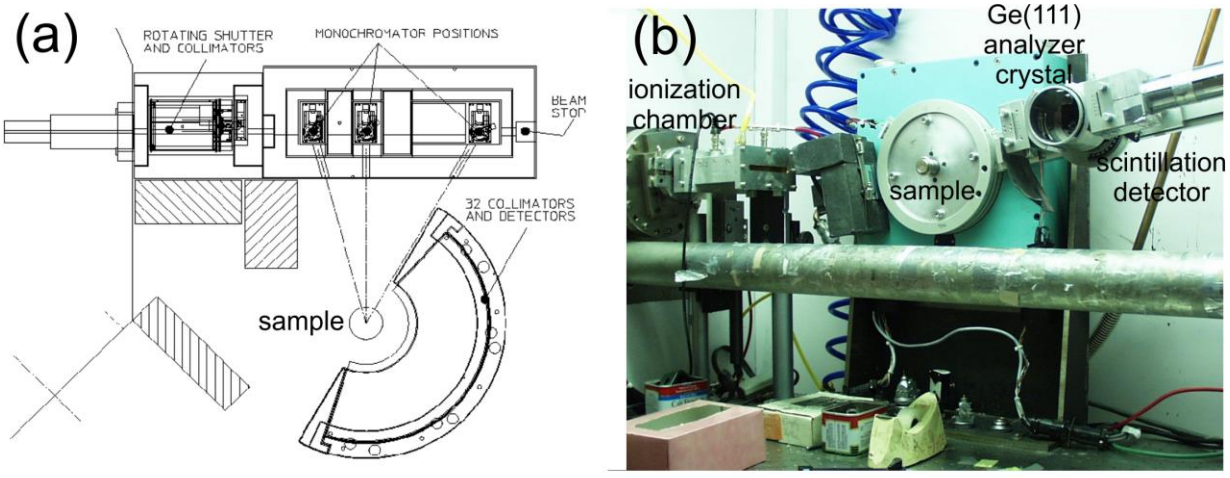

Figure from http://www.ncnr.nist.gov/instruments/bt1/bt1_plan.html

Photograph from http://www.ccp14.ac.uk/ccp/web-mirrors/pssp/X3B1overview.html

Figure 3: (a) The layout of the BT-1 high resolution neutron powder diffractometer at the NCNR, NIST. (b) The X3B1 synchrotron powder diffractometer at the NSLS, Brookhaven National Laboratory.

Polymorphism

Polymorphism is defined as the crystallization into two (or more) chemically identical, yet crystallographically distinct forms.[5] The different arrangements of atoms within crystals can have tremendous consequences on the physical properties. To illustrate this, consider the canonical example of two familiar allotropes of carbon, diamond and graphite. Diamond is the hardest known naturally occurring solid, it appears colorless and brilliant and it is a good electrical insulator, whereas graphite, commonly used in pencils, appears opaque, black, it is soft enough that a person of average strength can easily exert enough pressure on it to break it, and it is a semimetal.[6] These differences in physical properties are due to differences in chemical

bonding of the carbon atoms within each material, which leads to different spatial arrangements of atoms in the solids.

It is often the case that charge transfer salts, such as the ones studied in this work, exhibit polymorphism. Different polymorphs showing different physical properties can be synthesized by applying the technique of liquid assisted grinding (LAG), and this will be further explained in the Methods and Materials section.

Charge Transfer Salts

Oxford condensed matter physicist John Singleton authored an article in 2002, entitled "Why do physicists love charge transfer salts?", extolling the virtues of using charge transfer salts (CTS) to understand aspects of magnetism and superconductivity.[7] He argues that condensed matter physicists have ignored the potential uses of organic small molecules in experimentation due to the false assumption that fundamental physicists should study chemically simple materials.[7] In reality, despite being chemically complex, CTS often have beautifully simple electronic properties, with charge transferred anisotropically in one or two dimensions, as opposed to isotropic inorganic conductors.[7] Furthermore, CTS are being employed by physicists in an attempt to understand many-body effects, such as electron-electron and electron-phonon interactions, due to the experimental effective masses being (roughly) five times as large in CTS than in inorganic materials.[7]

Both compounds under study are organic charge transfer salts. This type of material is formed when electron donor molecules transfer electrons to electron acceptor molecules.[7] The charge transferred serves to keep the salt chemically bonded and also as a "dopant", by leaving

behind an empty electron state shared by the donor molecules.[7] The typical crystal packing motifs of tetrathiafulvalene donors in ionic and mixed-valence CTS are well known.[8] The knowledge of the crystal structure of a given compound often can be enough to deduce whether or not charge has been transferred.

This project sought to elucidate the crystal structure of two distinct CTS, TTF-2,5-dichloro-*p*-benzoquinone and TTF-*o*-CA, made of the components represented below.

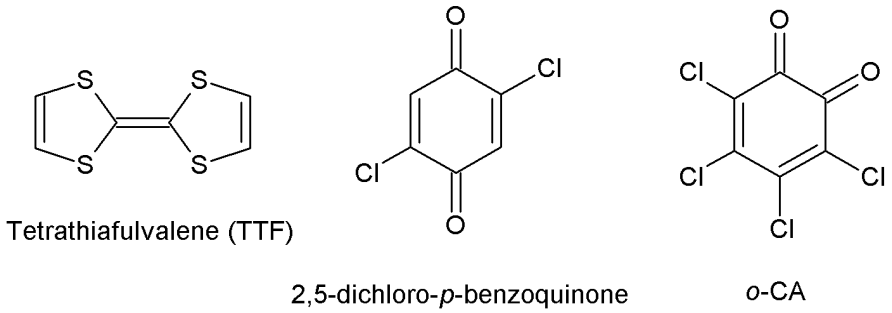

Figure 4: Molecular structures of the donor and acceptors in the TTF-2,5-dichloro-*p*-benzoquinone and TTF-*o*-CA charge transfer salts.

Specifically, the project focused on the crystal structure determination from powders of TTF-*o*-CA and the refinement of the crystal structure of TTF-2,5-dichloro-*p*-benzoquinone from their combined X-ray synchrotron and neutron powder diffraction data. For the latter, our work focused on the calculation of very accurate bond lengths in TTF to estimate the charge transferred, ρ, using empirical formulas.[9] A further objective of this project has been to better understand two new compounds, which may be used for purposes ranging from condensed matter physics studies to understanding aspects of mechanochemistry and crystal engineering.

2. Theory

This section aims to highlight the theoretical basis upon which powder diffraction relies, while highlighting the specific techniques and models that the data analysis section is based on.

The Crystalline State

Solids can be amorphous or crystalline. A crystal exhibits a long range periodic repetition of atoms (ions or molecules) with certain symmetry relations, and a periodic electron density distribution.[6] The unit cell is the "building block" of any crystal that repeats along the three spatial dimensions, and it has the same empirical formula and symmetry than the crystal. A unit cell (in three dimensions) is described by six lattice parameters: a, b, c, α, β, γ and the crystal system. The first three parameters describe the length of the unit cell edges, and the last three describe the angles between them. There are seven possible crystal systems: triclinic, monoclinic, orthorhombic, tetragonal, trigonal, hexagonal and cubic. Those are defined by minimum characteristic rotational symmetry elements of the crystal.[10]

A crystal lattice is an infinite array of points, each one surrounded equally by its neighbors,[10] and it can be generated by translations of three basis vectors **a, b, c**. A total of 14 types of unit cells, called Bravais lattices, describe all lattices used in crystallography. To understand how crystal structures are described, we imagine that the Bravais lattice is an abstract scaffold of lattice points, and that there is a set of atoms called the "asymmetric unit" (or "basis") associated with each lattice point. Once a Bravais lattice, the crystal symmetry and the

asymmetric unit are known, the crystal can be generated by simply translating the unit cell and its contents through the three spatial dimensions.

In the same way as individual molecules or other finite objects, crystals possess symmetry elements and a symmetry operation defined by each symmetry element. In crystals, symmetry elements with a translational component produce an infinite number of symmetrically equivalent objects, and they are called "infinite" symmetry elements. Examples of those are lattice translations, screw axes and glide planes.[4] The remaining symmetry elements which do not involve translations are called "finite" symmetry elements, such as inversion centers, mirror planes, rotation and roto-inversion axes.[4] Those elements can also be used to describe the symmetry of discrete objects such as molecules.

The complete set of symmetry elements of a crystal is called a "space group of symmetry", consistently with the mathematical theory of groups. A group is a set of elements for which a binary combination law is defined, and which together satisfy the four fundamental properties of closure, associativity, identity and inversion.[4] A total of 32 point groups exist if only finite symmetry elements and all their combinations are taken into account, whereas a total of 230 three-dimensional crystallographic space groups can be defined.[4]

Diffraction

Bragg's law expresses the necessary condition to observe diffracted radiation from a crystal. It states that constructive interference only occurs when the path difference ($2\,d \times \sin\theta$) between X-rays scattered by parallel lattice planes separated by an interplanar distance '*d*', is an integer number of wavelengths, *n*:

$$n\lambda = 2d\sin\theta \qquad (1)$$

where λ is the X-ray wavelength and θ is the angle of incidence of the X-rays on the crystal. Bragg's law is schematically represented in the figure below.

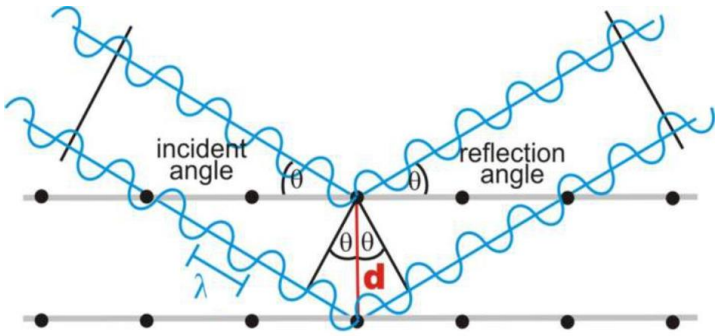

Figure from http://www.microscopy.ethz.ch/bragg.htm

Figure 5: Schematic representation of Bragg's law.

Although it might initially seem doubtful that small variations from an integer number of wavelengths would result in destructive interference, consider that after a small initial path difference, each additional plane again destructively interferes with parallel rays, for a (theoretically) infinite number of crystallographic planes. Thus, even a small variation of path difference from nλ would result in the absence of diffracted radiation. The wavelengths of incident X-rays commonly used in crystallography range from 0.5 to 2.5 Å,[4] which guarantees the scattering of the X-rays by the periodically arranged atoms in crystals, resulting in a diffraction pattern.

Reciprocal Space

Understanding the reciprocal space is essential to interpreting the diffraction pattern of a crystal. This is because each diffraction spot observed on a data collection plate (varies depending on the instrumentation used, can be photographic film or image plates) corresponds to the diffracted intensity from a lattice plane with interplanar spacing '*d*' as described above, labeled with particular Miller indices (h,k,l). In general several thousands spots will be measured within "frames" of data.[11] The reciprocal lattice can be understood by rearranging Bragg's law, and noticing the inverse relationship of the interplanar spacing, *d*, with sinθ. From this equation, we can infer that when a lattice has large *d* values the diffraction pattern will compress, while small *d* values will result in a wider spread.[11] Experimentally, when a lattice has long axes the diffraction spots tend to appear very close together, with the converse true for short axes.[11] If we assume that for each set of lattice planes in real space there is a point in the reciprocal space, then the collection of those points can be referred to as the reciprocal lattice.

We use the diffraction data which exists in the reciprocal space in order to define the crystal structure which exists, of course, in real space.[11] The data are ultimately used to calculate an electron density distribution map for the unit cell in real space.[11]

The Fourier Transform

In order to solve a crystal structure and to identify the positions of the atoms within the crystal, it is necessary to calculate the phases of the diffracted X-ray beams, also called structure factors. The "phase problem" as it is commonly referred to in crystallography, refers to the loss

of information about the phases of the diffracted X-rays, which intensities can be experimentally determined.

Returning to the process of 'seeing' things around us, the retina in the eyes is a lens that physically recombines the radiation scattered by visible objects so that an image of them can be formed. For X-rays diffracted by crystals, that recombination is not done by an X-ray lens but rather mathematically, using a method called Fourier synthesis.[11]

The structure factors for any reflection with Miller indices (h, k, l) are represented by **h**, have an amplitude $|F_{\mathbf{h}}|$ and a phase $\varphi_{\mathbf{h}}$, so each structure factor is:

$$F_{\mathbf{h}} = |F_{\mathbf{h}}| \exp(i\varphi_{\mathbf{h}}) \qquad (2)$$

The periodic electron density distribution ρ at any position **r** in a unit cell of volume V, is expressed in electrons per cubic Angstrom ($e^-/Å^3$), and it can be rebuilt by Fourier transform from the experimentally determined amplitudes of the structure factors and their calculated phases, through the following summation in **h**:

$$\rho(\mathbf{r}) = \frac{1}{V}\sum_{h} F_{\mathbf{h}} \exp[-2\pi i(\mathbf{h}.\mathbf{r})] \qquad (3)$$

Using equation (2) in the above formula gives:

$$\rho(\mathbf{r}) = \frac{1}{V}\sum_{h} |F_{\mathbf{h}}| \exp(i\varphi_{\mathbf{h}}) \exp[-2\pi i(\mathbf{h}.\mathbf{r})] \qquad (4)$$

In single crystal diffraction only the phases $\varphi_{\mathbf{h}}$ of the structure factors remain to be calculated. This is routinely done in the case of small organic molecules using the "direct methods" for crystal structure determination,[12] which use probability relations originating in properties of the electron density distribution function, its 'positivity' and the fact that it is centered around the atomic positions in the crystal. In other words, among all possible combinations of amplitudes and phases for the structure factors, a restricted number of them can generate an electron density distribution that is always positive and maximized at the atomic positions. This generates probabilistic relationships for the phase angles $\varphi_{\mathbf{h}}$ of triplets of reflections with arithmetically related Miller indices,[12] from which the phases can be calculated. However, these methods are considerably less successful for the determination of small organic structures from powder diffraction data due to peak overlap.

In powder diffraction, the specimen studied is a powder made of a large number of microcrystallites oriented at random. As a consequence of this, the three-dimensional information of the reciprocal lattice is lost, and the powder diffraction data only provides the '*d*' spacings (or $2\theta_{hkl}$ diffraction peak positions) of the Bragg reflections. In other words, only the magnitudes of the reciprocal lattice vectors. Consequently, in order to determine a crystal structure from powders, not only the phases of the reflections must be calculated, but the powder diffraction data does not provide individual measurements of the $|F_{\mathbf{h}}|$ due to the overlap of the diffraction peaks along the 2θ angle. Due to crystal symmetry, there are groups of reflections whose intensities can be independently measured in single crystal diffraction, but that are exactly overlapped at the same $2\theta_{hkl}$ angle. Though often those reflections have equal intensities, this is not always true. In addition, the diffraction peaks of reflections with close $2\theta_{hkl}$ angles partially overlap, and this problem is particularly severe at high diffraction angles.

The powder diffraction pattern is collected at small 2θ steps (typically 0.005° – 0.02°), and each observed diffracted intensity (called $y_{i,obs}$) at the Bragg angle $2\theta_i$ has contributions of various exactly and partially overlapped Bragg reflections.[13] Modern whole pattern decomposition methods[14] generate a set of calculated 'single crystal-like' integrated intensities for the reflections (sometimes called "pseudo-observed" integrated intensities) and structure factor amplitudes, that can later be used in crystal structure determination from powders to find the structure factor phases.

Direct Space Methods

Direct space methods refer to modern crystal structure determination techniques for powder samples, wherein the solution is found from a large number of trial models generated in the direct (or real) space. In 1989, Newsam and Deem[16] published a breakthrough crystal structure solution of a zeolite using the simulated annealing global optimization algorithm.[17] At present, direct space methods are implemented in various computer programs and have made use of other algorithms such as Monte Carlo, genetic algorithms and parallel tempering.[18-22]

In this work we have used the computer program PSSP (powder structure solution program).[22] The simulated annealing algorithm operates by minimizing a cost function 'S', which evaluates the difference between the integrated intensities calculated from each trial model with those generated in the Le Bail fit.[22]

Whole Powder Pattern Decomposition by the Le Bail method

Whole pattern decomposition is utilized in order to extract a set of integrated intensities for the Bragg reflections from the powder diffraction data, regardless of diffraction peak overlap. There are essentially two algorithms, the Le Bail method and the Pauli method.[14] In the Le Bail method, the unit cell parameters and the peak profile function are simultaneously refined and a set of the integrated intensities of the Bragg reflections is calculated from the measured powder diffractogram.[14]

The Le Bail method is based on iterating the Rietveld decomposition formula,[13] that has been initially used to partition each experimental powder diffraction intensity $y_{i,(obs)}$ at each position $2\theta_i$ of the powder diffraction pattern, into contributions to the several exactly overlapped and partially overlapped Bragg reflections centered at various $2\theta_{hkl}$ close to $2\theta_i$.

In the Rietveld method, the calculated powder diffraction intensity at each point of the powder pattern $y_{i,(calc)}$, is the product of the scale factor and a sum of the contributed intensities from the various overlapped Bragg reflections with peak maxima at $2\theta_{hkl}$ close to the position $2\theta_i$, plus the background intensity at that position:

$$y_{i,(calc)} = s\sum_{hkl} L_{hkl}\left|F_{hkl}\right|^2 \phi(2\theta_i - 2\theta_{hkl})P_{hkl}A + y_{b,i} \qquad (5)$$

where s is the scale factor, L_{hkl} is the product of the Lorentz factor, polarization factor, and multiplicity factor of the Bragg reflection of Miller indices h,k,l; $|F_{hkl}|^2$ is the structure factor amplitude square of each contributing reflection; ϕ is the peak shape function, that depends on the difference between $2\theta_i$ and $2\theta_{hkl}$ and it has integral equal to 1; P_{hkl} is the preferred orientation

correction for each reflection; A is the absorption correction for the specimen, and $y_{b,i}$ is the background intensity at that point of the powder pattern. The calculated intensity above the background can be written from equation (5) as:

$$y_{i,(calc)} = \sum_{hkl} w_{i,hkl} S^2_{(calc),hkl} \qquad (6)$$

where $w_{i,hkl}$ is a measure of the contribution of the Bragg reflection at $2\theta_{hkl}$ to the diffraction intensity $y_{i,(calc)}$ at the position $2\theta_i$ including the various factors detailed in (5), and $S^2_{(calc),hkl} = \left|F_{hkl}\right|^2$.

In the Rieveld method,[13] a partition of the the $y_{i,(obs)}$ for the calculation of 'observed' integrated intensities of the Bragg reflections, $I_{(obs),hkl}$, is done using the square of the structure factor amplitudes calculated from the structural model. In the equation of the Rietveld decomposition formula shown below, $S^2_{(calc),hkl} = \left|F_{hkl}\right|^2$

$$I_{(obs),hkl} = \sum_i (w_{i,hkl} S^2_{(calc),hkl} / y_{i,(calc)}) \times y_{i,(obs)} \qquad (7)$$

where $w_{i,hkl}$ has the meaning above described for equation (6). The sum is over all *i* steps at angles $2\theta_i$ with $y_{i,(obs)}$ which can theoretically contribute to the integrated intensity $I_{(obs),hkl}$ of the diffraction peak at $2\theta_{hkl}$.

In other words, the observed intensities $y_{i,(obs)}$ at each point of the powder pattern are partitioned into contributions for the integrated intensities of the overlapped Bragg reflections (or

peaks) with Miller indices h,k,l, according to the partition (or 'construction' from the contributing Bragg reflections) of the calculated intensity at that point in the pattern, $y_{i,(calc)}$.

In the Le Bail method,[14] the $S^2_{(calc),hkl}$ are initially set to all equal arbitrary numbers, since the $|F_{hkl}|^2$ are not known, the scale factor is kept at a fixed value, and the Rietveld decomposition formula in (7) is iterated, so that the resulting $I_{(obs),hkl}$ are re-injected in subsequent iterations as the new $S^2_{(calc),hkl}$.

Figure 6 shows schematically the partition of the observed powder intensities $y_{i,(obs)}$ according to the fractional contributions to the calculated intensity $y_{i,(calc)}$ at each $2\theta_i$ step.

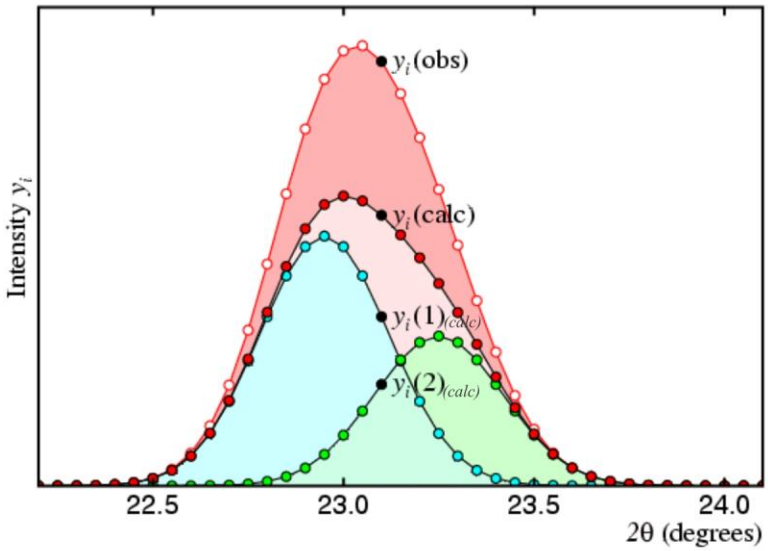

Figure from http://pd.chem.ucl.ac.uk/pdnn/solve1/lebail.htm

Figure 6: The experimental powder diffraction intensity at each step $y_{i,(obs)}$ is partitioned between the two overlapped diffraction peaks (1), (blue), and (2) (green) in this figure in particular, using the ratios $y_i(1)_{(calc)}/y_{i,(calc)}$ and $y_i(2)_{(calc)}/y_{i,(calc)}$ at each $2\theta_i$ step. In addition, $y_{i,(calc)}=y_i(1)_{(calc)} + y_i(2)_{(calc)}$; $y_i(1)_{(calc)} = w_{i,1} S^2_{(calc),1}$ and $y_i(2)_{(calc)} = w_{i,2} S^2_{(calc),2}$.

This project made extensive use of the Le Bail method. In order to utilize this method, it is important to have a good starting unit cell and profile parameters as in the Rietveld method itself.[4]

Rietveld Refinement

The Rietveld method relies upon a model for the crystal structure, in other words, a crystal structure solution containing atomic coordinates, lattice parameters, and space group symmetry. It allows us to establish structural details still missing from the *ab-initio* structure solution process.[4] Least squares refinements are carried out varying selected parameters until the best fit is obtained between the observed and calculated diffraction intensities at each point y_i at $2\theta_i$ of the powder profile. The crystallographic model (including atomic positions and lattice parameters), scale factor, background intensities, peak profile parameters, preferred orientation parameters, instrumental factors and diffraction optics effects (2θ zero error in the position of the detector, sample holder shift, transparency, X-ray absorption) can be refined from initially approximate models.[15]

3. Methods and Materials

Diffraction data collection

The study of the crystal structure of TTF-*o*-CA was conducted through X-ray powder diffraction. The high resolution X-ray powder diffraction data of TTF-*o*-CA and TTF-2,5-dichloro-*p*-benzoquinone were collected at room temperature in the beamline X16C of the

National Synchrotron Light Source, Brookhaven National Laboratory, NY, USA. The samples were loaded into 1 mm and 1.5 mm glass capillaries, respectively. The wavelength λ = 0.669711 Å was selected with a Si(111) double monochromator and the incident beam was monitored with an ion chamber. A Ge(111) analyzer crystal was placed after the sample and before the detector to obtain good angular resolution, whereas the out-of-plane resolution was given by slits. A NaI(Tl) scintillation detector was used to measure the diffracted radiation.

The study of the crystal structure and charge transfer of TTF-2,5-dichloro-*p*-benzoquinone was conducted through X-ray synchrotron and neutron diffraction from powders. The neutron powder diffraction data at constant wavelength was collected from the BT1 High Resolution neutron powder diffractometer at the NIST Center for Neutron Research, Gaithersburg, MD. The sample was loaded under He atmosphere into a vanadium can and the data was collected at room temperature over the range of 2θ=1.3-166.3° at constant 2θ steps of 0.05°. The 2.0787(2) Å wavelength was selected using a Ge (311) monochromator with a 75° take-off angle. The diffracted radiation was measured with 32 ^{3}He detectors at 5° intervals.

Synthesis

The synthesis conditions for the preparation of samples of the materials studied are summarized in the following paragraphs.

TTF-2,5-dichloro-*p*-benzoquinone:

0.9650 g of TTF were ground with 0.8357 g of 2,5-dichloro-*p*-benzoquinone and 7.20 mL of acetonitrile (MeCN) for 40 minutes in a glass mortar with pestle, under air and at room

temperature. The ratio of solvent to reactant mass was 4 μL per mg. The color of the resulting product was green.

TTF-*o*-CA

0.0113 g of TTF (orange, monoclinic polymorph) were ground with 0.0136 g of *o*-CA (ortho-chloranil) and 25 μL of toluene in an agate mortar with pestle, under air and at room temperature for 30 minutes total. After the first 15 minutes of grinding, an additional volume of 25 μL of toluene was added and the grinding continued for additional 15 minutes. The color of the resulting product was pink.

Diffraction data analysis

The table below offers a rough outline of the process of analyzing X-ray powder diffraction data.

Table 2: Outline of the procedure for the Crystal Structure Determination from Powders

Step (#)	Operation	Information gained
Step (1)	Preparation of a powder specimen	X-ray absorption, sample transparency and preferred orientation effects must be minimized.
Step (2)	Data collection	Powder diffraction data, as a list of $y_{i,obs}$ *vs.* $2\theta_i$
Step (3)	Data reduction	Estimation of background intensities and $2\theta_{hkl}$ peak positions.

Step (4)	Obtain unit cell (indexing)	Crystal system, unit cell parameters (a, b, c, α, β, γ) and unit cell volume.
Step (5)	Obtain space group symmetry	Space group symmetry
Step (6)	Whole powder pattern decomposition	A set of calculated I_{obs} for the reflections, refined unit cell parameters and peak profile function.
Step (7)	Structure solution (direct space methods or other).	Approximate non-Hydrogen atomic positions.
Step (8)	Rietveld refinement	Final atom positions including calculated Hydrogen positions. Atomic thermal displacement parameters and other non-crystallographic parameters.
Step (9)	Interpretation of the results	Molecular geometry, crystal packing motif and chemical bonding.

Application of Crystallographic Software

Data reduction and indexing

The computer program WinPLOTR[23] was used to represent graphically the diffraction data of both compounds and to identify powder diffraction peaks.

DICVOL[24] is an indexing program working through an exhaustive search of lattice parameters by the successive dichotomy method.[4] In addition to DICVOL, the programs ITO[25] and TREOR[26] were also used. ITO utilizes a zone search indexing method combined with the Delaunay-Ito technique in order to determine the most probable unit cell.[4] TREOR[26] is a semi-exhaustive trial and error indexing program, based on the permutation of Miller indices in a basis set of low angle reflections.[26] These programs allow the optional input of information about the formula weight and density in order to estimate the number of formula units expected in the unit cell found. This process is called *ab-initio* indexing, since the lattice parameters are not known *a-priori*. Other program used is McMAILLE.[27] At this point, it may be possible to determine the space group symmetry by noting that certain subsets of reflections have zero intensity, which is an effect of the presence of symmetry elements with a translational component.[4]

Space Group Symmetry Determination

The computer program EXPO[28] was utilized to determine the space group symmetry. The program reads the raw diffraction data file, the X-ray source (*e.g.*, synchrotron), with the option of including known lattice parameters or finding them from peak positions as well. The program produces a list of most likely space groups of symmetry for the material, with figures of merit (FOM) attached to each of them. The lattice parameters and space group symmetry are used to extract a set of integrated intensities for the reflections through the Le Bail algorithm, implemented in the computer programs GSAS[29] or FULLPROF.[30]

Crystal Structure Solution

The refined lattice parameters, space group symmetry and a file with the integrated intensities of the reflections, are utilized by the Powder Structure Solution Program (PSSP)[22] to find the crystal structure solution (approximate atomic coordinates). PSSP uses the simulated annealing global optimization algorithm[17] to sort the structure solution from thousands or millions of possible atomic arrangements calculated. The algorithm works by minimizing a cost function, which mathematically expresses the difference between the integrated intensities calculated from any trial model, and correlated integrated intensities extracted in the Le Bail fit of the experimental pattern.[22] Each simulated annealing run results in a set of approximate atomic coordinates, which then must be refined by the Rietveld method in order to reach a publishable crystal structure solution.

Rietveld Refinement

The knowledge of the approximate atomic positions allows us to perform a Rietveld refinement on the atomic positions defining the structural model.[13,15] In the Rietveld method the integrated intensities of the reflections are calculated from the structure factors (which contain the atomic positions), thus they are biased by the structural model. The program GSAS[29] allows to include bond distance and bond angle restraints in the Rietveld refinement process, which affords the calculation of chemically meaningful structures.

Statistical Significance and Data Presentation of the results

Three agreement factor values are most commonly utilized in order to test the validity of the crystallographic data obtained from the structure solution process from powders: R_{wp} (R-weighted pattern), R_I (R-Bragg factor) and χ^2 or goodness of fit (GOOF) squared. During the Rietveld refinement process, the R_{wp} factor and χ^2 are often used as a monitor of the progress of the refinement cycles.

$$R_{wp} = \left\{ \frac{\sum_i w_i (y_{i,obs} - y_{i,calc})^2}{\sum_i w_i (y_{i,obs})^2} \right\}^{1/2} \quad ; \text{where } w_i = 1/y_{i,\,obs} \tag{8}$$

The goodness of fit is defined as:

$$\chi = \frac{R_{wp}}{R_{\exp}} \tag{9}$$

and R-expected (R_{exp}) is defined as:

$$R_{\exp} = \left[(N - P) / \sum_i w_i y_{i,obs}^2 \right]^{1/2} \tag{10}$$

where N is the number of profile points (*i*) and P is number of Rietveld parameters.

The R_I (or R-Bragg factor) is defined as:

$$R_I = \frac{\sum_{hkl} \left| I_{(obs),hkl} - I_{(calc),hkl} \right|}{\sum_{hkl} I_{(obs),hkl}} \tag{11}$$

where $I_{(obs),\,hkl}$ and $I_{(calc),\,hkl}$ are the 'observed' and calculated integrated intensities of the Bragg reflections (peaks) with Miller indices h,k,l.

The agreement factors above provide a better overall view of the convergence of the refinement and they are useful in determining whether a model is correct.

4. Results

TTF-*o*-CA

The crystallographic data of TTF-*o*-CA is shown in table 3. The unit cell parameters were found with DICVOL[24] and the most likely space group symmetry $P2_1/n$ was determined with the program EXPO.[28] A set of integrated intensities for the reflections was extracted with the program GSAS.[29] The Cartesian coordinates utilized for crystal structure solution were taken from another polymorph of TTF-*o*-CA.[31] The program PSSP[22] was run using the integrated intensities of the first 225 reflections and 250,000 models per temperature (1.225×10^7 total trial models). However, the analysis of the crystallographic models obtained did not provide a conclusive result for the crystal structure solution.

Table 3. Crystallographic Data of TTF-*o*-CA

Lattice parameters	a = 12.1332(8) Å b = 13.1388(7) Å c = 10.6180(6) Å α = 90˚, β = 108.447(4)˚, γ = 90˚
Unit cell volume	1605.71(17) $Å^3$
Space group symmetry	$P2_1/n$
Empirical formula	$C_{12}H_4Cl_4O_2S_4$
Z	4
Molecular weight (amu)	450.2
Crystal system	Monoclinic
R_{wp}, χ^2	11.26%, 1.076

The Le Bail fit of the synchrotron diffraction data is shown in figure 7.

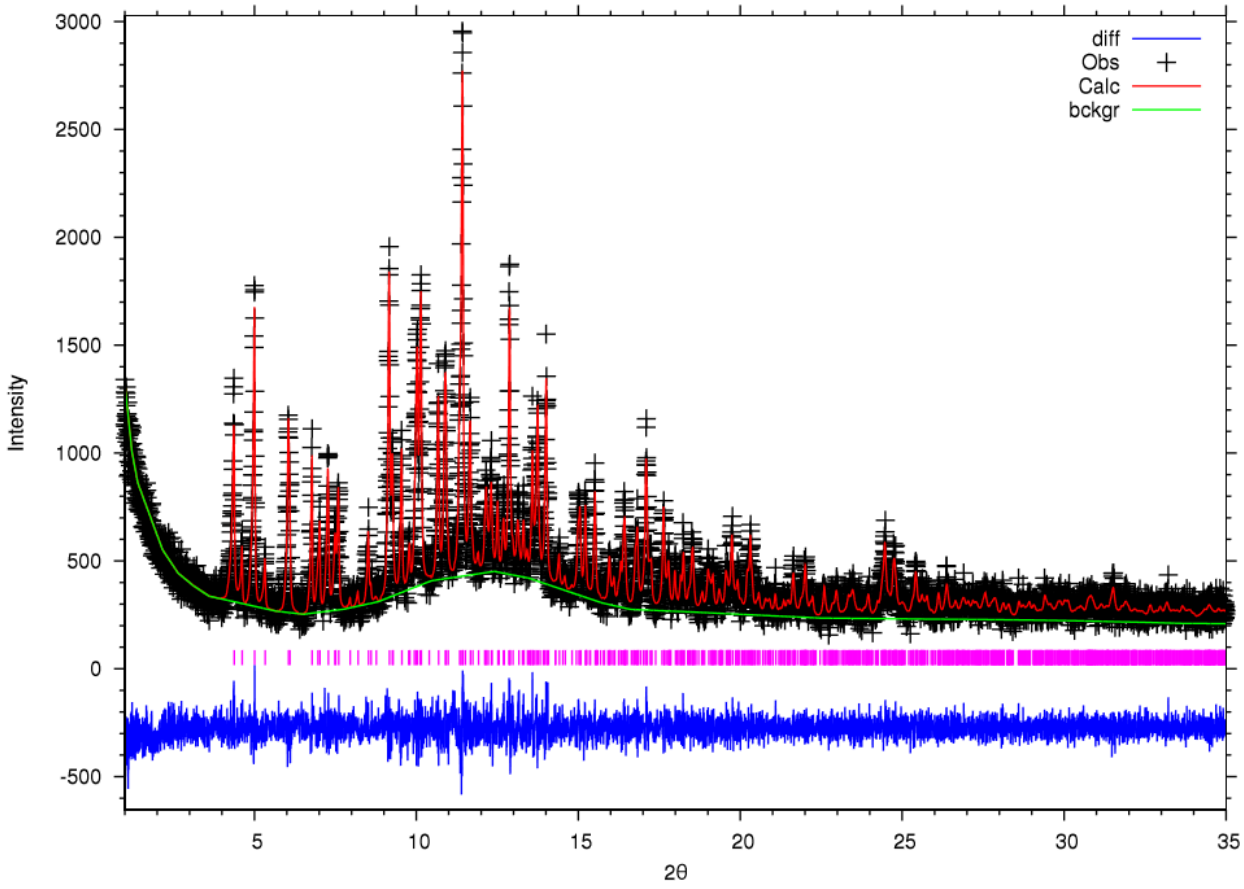

Figure 7. Le Bail fit of the synchrotron X-ray powder diffraction data of TTF-*o*-CA. The experimental data is represented with (+), the calculated profile is shown with a solid red line, the background intensity is shown with a solid green line and the difference of the observed and calculated profiles is represented with a solid blue line. Pink tick marks show the positions of the Bragg reflections.

TTF-2, 5-dichloro-*p*-benzoquinone

The crystallographic data of TTF-2,5-dichloro-*p*-benzoquinone is summarized in table 4. The Rietveld fits of the neutron powder diffraction data and the synchrotron X-ray powder diffraction data are shown in the figures 8 and 9, respectively. Both datasets were simultaneously fitted by the crystallographic model refined. In the final Rietveld cycles the following parameters were refined: unit cell parameters, thermal displacement parameters, background coefficients (both datasets), zero point error in the detector (both datasets), and scale factors. Other parameters previously refined have been the peak profile parameters and preferred orientation parameters (both datasets).

The molecular geometries of TTF and 2,5-dichloro-*p*-benzoquinone were refined subjected to bond length, bond angle restraints and planarity restraints using GSAS.[29] The values for the restraints were obtained from Le Cointe *et al.*[9] for the room temperature structure of TTF-CA from single crystal neutron diffraction data.

Table 4. Crystallographic Data of TTF-2,5-dichloro-*p*-benzoquinone

Lattice parameters	a = 9.7665(3) Å, b = 11.1449(4) Å, c = 7.21387(18) Å α = 97.702(2)˚, β = 104.791(2)˚, γ = 98.5339(19)˚
Unit cell volume	738.55(4) Å^3
Space group symmetry	$P\bar{1}$
Empirical formula	$C_{12}H_6Cl_2O_2S_4$
Z	2
Molecular weight (amu)	381.3
Crystal system	Triclinic
R_{wp} (totals) R_{wp} (neutron diffraction) R_{wp} (X-ray diffraction) χ^2 R_I	2.71% 1.43% 8.63% 1.720 3.72%

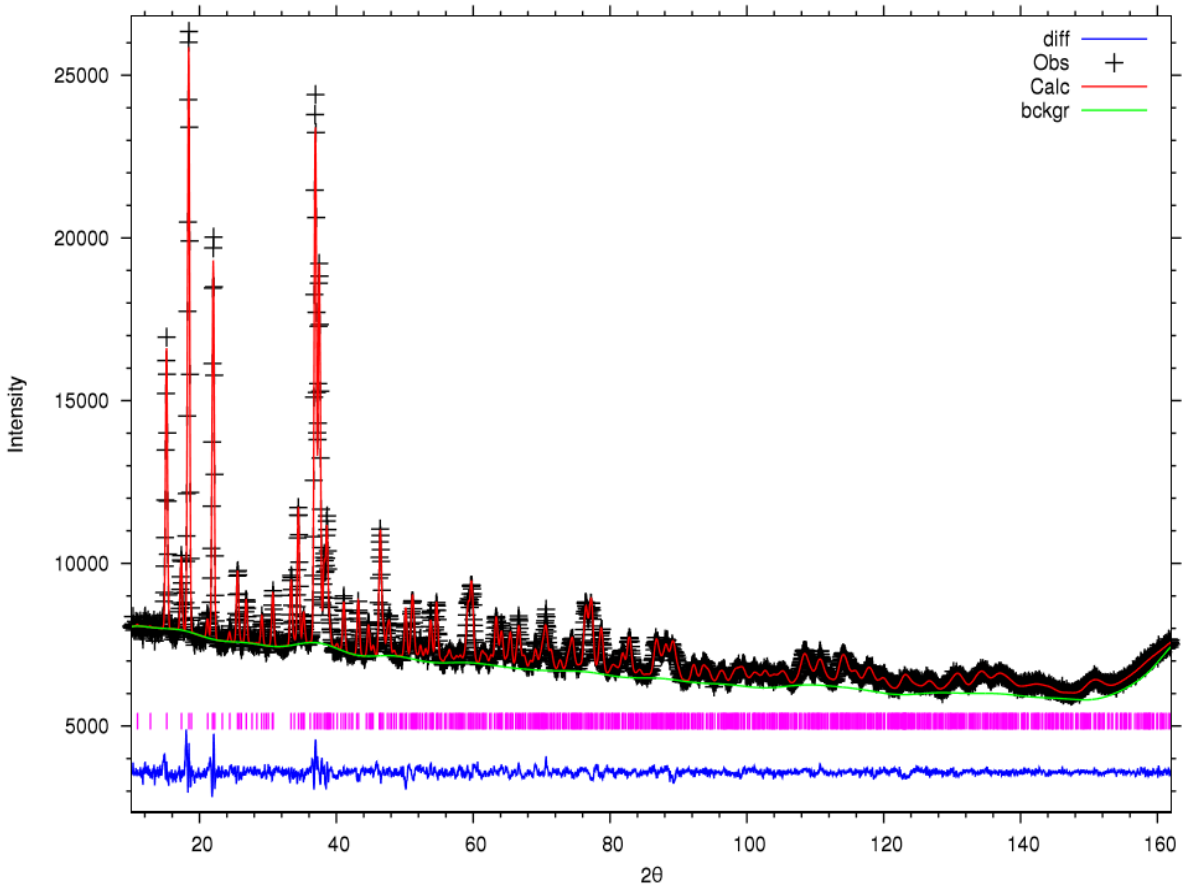

Figure 8. Rietveld fit of the neutron powder diffraction data of TTF-2,5-dichloro-*p*-benzoquinone. The experimental data is represented with (+), the calculated profile is shown with a solid red line, the background intensity is shown with a solid green line, and the difference of the observed and calculated profiles is represented with a solid blue line. Pink tick marks represent the positions of the Bragg reflections.

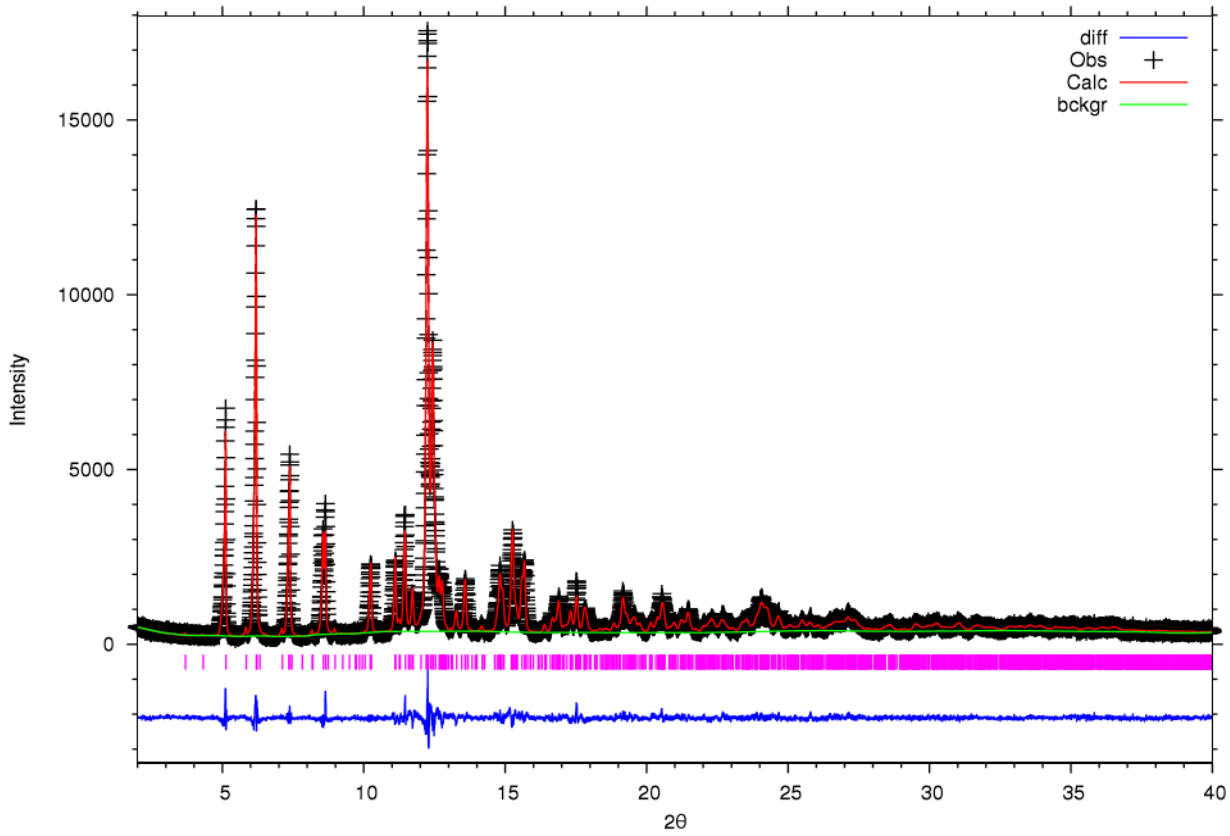

Figure 9. Rietveld fit of the synchrotron X-ray powder diffraction data of TTF-2,5-dichloro-*p*-benzoquinone. The experimental data is represented with (+), the calculated profile is shown with a solid red line, the background intensity is shown with a solid green line, and the difference of the observed and calculated profiles is represented with a solid blue line. Pink tick marks represent the positions of the Bragg reflections.

Crystal Structure Validation

Although the above lattice parameters, space group symmetry and atomic coordinates demonstrate a strong correspondence to the experimental data and good Rietveld refinements were obtained, the crystal structure still required validation by checking for errors that were hidden in the structure determination process. The structure of TTF-2,5-dichloro-*p*-benzoquinone was initially solved with two formula units per unit cell (Z=2), however it was later discovered through the use of the crystal structure validation program PLATON,[32] that the volume of the

initial unit cell found at the indexing step was unnecessarily duplicated, and there is one formula unit per unit cell (Z=1) and inversion symmetry in the TTF and 2,5-dichloro-*p*-benzoquinone molecules. PLATON[32] checks for missing symmetry - often difficult to find at the initial stages of a structure solution. The corrected structural description is summarized in the table 5.

Table 5. Validated Crystallographic Data of TTF-2,5-dichloro-*p*-benzoquinone

Lattice parameters	a = 6.841764(2) Å, b = 7.213306(17) Å, c = 7.934819(2) Å α = 93.618(17)˚, β = 97.627(19)˚, γ = 106.941(19)˚
Unit cell volume	369.147(17) Å^3
Space group symmetry	$P\bar{1}$
Empirical formula	$C_{12}H_6Cl_2O_2S_4$
Z	1
Molecular weight (amu)	381.3
Crystal system	Triclinic
R_{wp} (totals) R_{wp} (neutron diffraction) R_{wp} (X-ray diffraction) χ^2 R_I	2.58% 1.37% 7.8% 1.441 2.1%

The validated structure is now used to describe the packing of the molecules in the crystal. TTF-2,5-dichloro-*p*-benzoquinone is made of columnar stacks of alternating TTF and 2,5-dichloro-*p*-benzoquinone molecules, which extend along the direction of the *b*-axis. This packing motif is represented in the figure 10 (a). Adjacent columns are bonded in the crystal through weak hydrogen bonds and non-covalent interactions between pairs of sulfur atoms, forming layers. This can be seen from a direction parallel to the *b*-axis shown in the figure 10 (b).

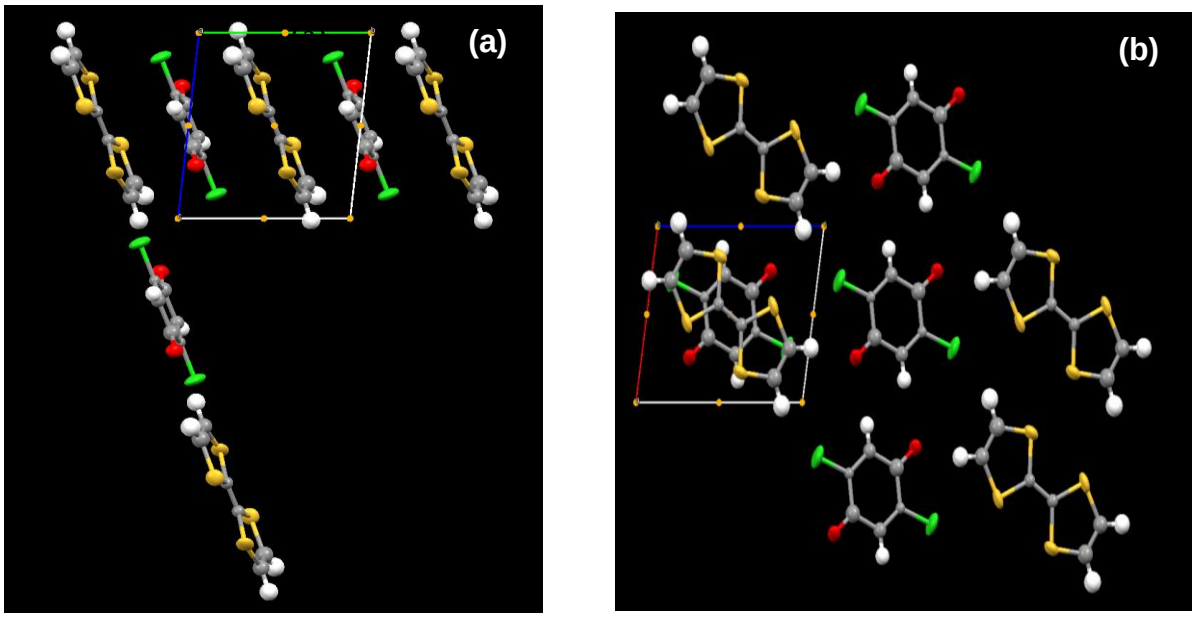

Figure 10. (a) A column of alternating TTF and 2,5-dichloro-*p*-benzoquinone molecules in the crystal structure of TTF-2,5-dichloro-*p*-benzoquinone, extending along the direction of the b-axis (shown in green). (b) Layers of TTF and 2,5-dichloro-*p*-benzoquinone with weak hydrogen bond formation and sulfur-sulfur non covalent interactions, viewed from a direction parallel to the b-axis. Representations generated by the program Mercury.[33] S=yellow, C=grey, Cl=green, O=red and H=light grey.

Charge Transferred in TTF-2,5-dichloro-*p*-benzoquinone

M. Le Cointe *et al.*[9] cite two empirical formulas to calculate charge transferred for organic CTS. The first formula is more reliable than the second one.

Formula 1: $\rho = -15.55 + 20.42 \times (r/s)$

Formula 2: $\rho = 4.49 + 10.748 \times (r-s)$

In both formulas r equals to the central C=C bond distance in TTF and s is the average of the four adjacent C-S distances. Both formulas have been derived from a series of organic CTS structures containing TTF.[9]

Using the bond lengths refined with the Rietveld method for TTF-2,5-dichloro-*p*-benzoquinone a charge transfer can be calculated. According to the formula 1:

$\rho = -15.55 + 20.42 \times (1.361 \text{ Å}/1.74725 \text{ Å}) = 0.36 \text{ e}^-$,

and from the formula 2:

$\rho = 4.49 + 10.748 \times (r-s) = 0.34 \text{ e}^-$

5. Discussion

The Rietveld fit of the synchrotron and neutron powder diffraction data of TTF-2,5-dichloro-*p*-benzoquinone has acceptable agreement factors of R_{wp} = 2.58%, R_I = 2.1 % and χ^2 = 1.441. The charge transferred (ρ) was calculated to be approximately ~0.36 e^-. It is important to note that these values may be biased by the bond length restraints and another experimental technique should be used to further validate them (*e.g.* infrared spectroscopy). Based on the packing motif of the compound, as shown in figure 10, the compound cannot be an organic metal since it has columns made of alternating TTF and 2,5-dichloro-*p*-benzoquinone, which are typical of semiconductors/insulators. Moreover, the space group $P\bar{1}$ is not compatible with ferroelectricity.

For TTF-*o*-CA, the χ^2 from the Le Bail fit obtained is acceptable (as shown in figure 7), which indicates the correctness of the lattice parameters. However, the results from the structural solution runs are inconclusive due to the lack of repetition of a crystal packing motif that is chemically plausible within the solution set with the best agreement factors. There are a few likely causes for this, such as incorrect space group symmetry or wrong parameterization of the structure. In order to solve this structure, the next steps that should be taken include re-examination of the space group symmetry, and a new parameterization of the structure with more than one crystallographically independent TTF, *o*-CA or both fragments.

Acknowledgements

We acknowledge the support of the National Institute of Standards and Technology, U. S. Department of Commerce, in providing the neutron research facilities used in this work.

We acknowledge synchrotron powder diffraction data collected at the beamline X16C of the National Synchrotron Light Source. Use of the National Synchrotron Light Source, Brookhaven National Laboratory, is supported by the U.S. Department of Energy, Office of Science, Office of Basic Energy Sciences, under Contract No. DE-AC02-98CH10886.

Funding from the International Center for Diffraction Data (ICDD) GIA 08-04 is gratefully acknowledged.

Finally, SHM is profoundly grateful for the untiring guidance and support of Dr. Silvina Pagola throughout the thesis process, who shared her deep love of chemistry and science with a contagious enthusiasm.

References

1. (a) "Democritus on the Atom." *Scientific American* (1949), *181(5),* 48-49. (b) Russell, B. "A History of Western Philosophy." Simon and Schuster, New York, 1972.
2. Eckert, M. "Max von Laue and the discovery of X-ray diffraction in 1912". *Ann. Phys.* (Berlin) (2012), *524*, A83–A85.
3. Louër, D. "Advances in Powder Diffraction Analysis." *Acta Cryst.* (1998) *A54,* 922-933.
4. Pecharsky, V. K. and Zavalij, P. Y. "Fundamentals of Powder Diffraction and the Structural Characterization of Materials". Kluwer Academic, Boston, 2003.

5. Gavezzotti, A. and Filippini, G., “Polymorphic Forms of Organic Crystals at Room Conditions: Thermodynamic and Structural Implications”, *J. Am. Chem. Soc.* (1995), *117*, 12299-12307.
6. Kittel, C. “Introduction to Solid State Physics”. 7th edition, John Wiley & Sons, New York, 1996.
7. Singleton, J. "Why Do Physicists Love Charge Transfer Salts?" *J. Solid State Chem.* (2012), *168*, 675-689.
8. Fourmigué, M. and Batail, P. “Activation of Hydrogen- and Halogen-Bonding Interactions in Tetrathiafulvalene-Based Crystalline Molecular Conductors,” *Chem. Rev.* (2004), *104*, 5379−5418.
9. Le Cointe, M., Lemée Cailleau, M. H., Cailleau, H., Toudic, B., Toupet, L., Heger, G., Moussa, F., Schweiss, P., Kraft, K. H. and Karl, N. "Symmetry Breaking and Structural Changes at the Neutral-to-ionic Transition in Tetrathiafulvalene-*p*-chloranil." *Phys. Rev.* (1995), *B51*, 3374-3386.
10. Atkins, P. W. “Physical Chemistry”, 4th edition, W. H. Freeman and Co., New York, 1990.
11. Clegg, W., “Crystal structure determination”, Oxford Chemistry Primers No. 60, Oxford University Press, UK, 1998.
12. Massa W., “Crystal structure determination”, Springer-Verlag, Germany, 2000.
13. Rietveld, H. M. "A Profile Refinement Method for Nuclear and Magnetic Structures." *J. Appl. Cryst.* (1969), *2*, 65-71.
14. Le Bail, A. “Whole powder pattern decomposition methods and applications: a retrospection,” *Powder Diffraction* (2005), *20*, 316-326.

15. Young, R. A., “The Rietveld Method”, IUCr Monographs on Crystallography, Oxford Science Publications, Oxford, UK, 1993.
16. Deem M. W. and Newsam, J. M.. *Nature* (1989), *342*, 260-262.
17. Kirkpatrick, S., Gelatt, C. D. and Vecchi, M. P. "Optimization by Simulated Annealing". *Science* (1983), *220*, 671-680.
18. David, W. I. F. and Shankland, K. "Structure Determination from Powder Diffraction Data”. *Acta Cryst.* (2008), *A64*, 52-64.
19. Harris, K. D. M. and Tremayne, M. "Crystal Structure Determination from Powder Diffraction Data." *Chem. Mater.* (1996), *8*, 2554-2570.
20. Chernyshev, V. V., “Structure determination from powder diffraction”, *Russ. Chem. Bull., Int. Ed.,* (2001), *50,* 2273-2292.
21. Černý, R. and Favre-Nicolin, V., “Direct space methods of structure determination from powder diffraction: principles, guidelines and perspectives”, *Z. Kristallogr.* (2007), *222*, 105-113.
22. Pagola S. and Stephens, P. W., *J. Appl. Cryst.* (2010), *43,* 370-376.
23. Roisnel, T., and Rodriguez-Carvajal, J.. Program WinPLOTR (2011). Downloadable from http://www.cdifx.univ - rennes1.fr/winplotr/winplotr.htm.
24. Boultif, A. and Loüer, D. *J. Appl. Cryst.* (2004), *37*, 724-731.
25. Visser, J.. *J. Appl. Cryst.* (1969), *2*, 89-95.
26. Werner, P. E., Eriksson, L. and Westdahl, M.. *J. Appl. Cryst.* (1985), *18*, 367-370.
27. Le Bail, A.. *Powder Diffraction* (2004), *19*, 249-254.
28. Altomare A., Caliandro, R., Camalli, M., Cuocci, C., Giacovazzo, C., Moliterni, A. G. G. and Rizzi, R.. *J. Appl. Cryst.* (2009), *42*, 1197-1202.

29. Larson, A. C. and Von Dreele, R. B.. Program GSAS (2004). Los Alamos National Laboratory report LAUR 86-748.
30. Rodriguez-Carvajal, J. *Physica B* (1993), *192*, 55.
31. Rosokha, S. V., Dibrov, S. M., Rosokha T. Y. and Kochi, J. K.. *Photochem. Photobiol. Sci.*, (2006), *5*, 914–924.
32. Spek, A. L., *Acta Cryst.* (2009), *D65*, 148-155.
33. Macrae, C. F., Edgington, P. R., McCabe, P., Pidcock, E., Shields, G. P., Taylor, R., Towler, M. and van De Streek, J. *J. Appl. Cryst.* (2006), *39*, 453-457.